A novel method to improve the gas storage capacity of ZIF-8

ARTICLE *in* JOURNAL OF MATERIALS CHEMISTRY · MAY 2012

Impact Factor: 7.44 · DOI: 10.1039/C2JM31541F

6 AUTHORS, INCLUDING:

Bei Liu
China University of Petroleum
73 PUBLICATIONS **970** CITATIONS
SEE PROFILE

Chang-Yu Sun
China University of Petroleum
107 PUBLICATIONS **1,274** CITATIONS
SEE PROFILE

Journal of Materials Chemistry

Dynamic Article Links

Cite this: *J. Mater. Chem.*, 2012, **22**, 12246

www.rsc.org/materials

PAPER

A novel method to improve the gas storage capacity of ZIF-8†

Liang Mu, Bei Liu,* Huang Liu, Yuntao Yang, Changyu Sun and Guangjin Chen

Received 13th March 2012, Accepted 24th April 2012
DOI: 10.1039/c2jm31541f

In this work a novel method for enhancing the gas storage capacity of metal–organic frameworks (MOFs), *i.e.* saturating the MOF with a suitable quantity of water and forming hydrates in it, was proposed. Commercialized ZIF-8 was adopted as it is very stable under an atmosphere of water. The adsorption and hydrate formation behaviors of methane in wet ZIF-8 with five different water contents (0.0%, 16.3%, 27.7%, 30.6%, and 35.1%, mass percentages) were investigated under hydrate formation conditions and the storage capacities of both ZIF-8 frameworks and ZIF-8 particle beds were determined. Our results show that hydrates can form in wet ZIF-8 pores and thus increase the overall storage capacities of both ZIF-8 frameworks and ZIF-8 particle beds remarkably. The contribution of hydrates to the total gas uptake of a ZIF-8 framework can be as high as 45%. Compared with dry ZIF-8 frameworks, the net storage capacity of the wet analogue with a water content of 35.1% increases from 5.954 to 9.304 mmol g^{-1} at 269.15 K and 2.85 MPa, in other words, raised by more than 56%. The ideal volume storage capacity of the wet ZIF-8 framework can achieve more than 190 V/V at 3.0 MPa or so, 7% higher than the DOE target (180 V/V) for methane storage. In addition, our SEM measurements and XRD analysis demonstrate that ZIF-8 is stable during the saturation and hydrate formation processes, illustrating that it can be used repeatedly.

1. Introduction

Natural gas which primarily consists of methane is a clean energy with a much lower carbon emission upon combustion. However, it cannot be stored at the same density as liquid fuels. Therefore, how to effectively, economically, and safely store natural gas at moderate temperatures and pressures has drawn much attention in past decades. Among many approaches proposed, physisorption in porous materials with large surface areas seems promising. To motivate research and development of methane storage materials, in 2000, the US Department of Energy (DOE) has set the target[1] for adsorbed methane storage as 180 V(STP)/V (STP: 298 K, 0.1 MPa) at 3.5 MPa and 298 K. Recently, many investigations regarding methane adsorption storage in different porous materials have been reported.[2–7] Numerous porous materials, such as active carbons,[8–11] single-walled carbon nanotubes,[12–15] zeolites,[16] graphite nanofibers,[17] and metal–organic frameworks (MOFs)[18–23] have been synthesized, investigated, and evaluated as adsorbents correspondingly. Though few of them can meet the DOE target, several MOFs have already been synthesized that exceed the value,[24] *i.e.* 180 V(STP)/V. Their results reveal that MOFs are a promising candidate for methane adsorption storage, encouraging us to carry out a study to try to enhance the methane storage capacity of MOFs further and utilize them more effectively. It should be noted that the cyclic and water stability of MOFs is very important in practical applications as water exists ubiquitously. As pointed out by Sayari and Belmabkhout,[25] the lifetime of adsorbents is a critical property of equal importance as gas adsorption capacity on the economics of any commercial scale operation. Unfortunately, although most MOFs have good thermal stability, a large number decompose upon contact with humid air.[26,27] The labile nature of many metal–oxygen bonds can lead to hydrolysis of the network thus irreversibly destroying the structure. One subclass of MOFs, zeolitic imidazolate frameworks (ZIFs) have however been tested to be water and even acid stable, thereby showing great potential in practical applications.[28,29] Although the presence of water has negative effect on most of MOFs, it may have positive effect for some porous materials. Sayari and Belmabkhout have demonstrated that by using moisture-containing gases, the stability of some adsorbents as well as the gas uptake, especially CO_2 uptake in amine functionalized porous materials, can be enhanced.[25]

Besides physisorption in porous materials, storage of gas in the form of a hydrate is another promising approach. It is well known that natural gas and water can form a gas hydrate under suitable temperature and pressure. In reference to standard conditions, natural gas hydrates can contain 176 volumes of gas per volume of hydrate (V/V) in theory.

By investigating the adsorption behavior of gas in the pores of porous materials, we found that part of the pore volume is not used effectively in most cases. We therefore considered forming a suitable quantity of hydrate in the pores of materials to increase

State Key Laboratory of Heavy Oil Processing, China University of Petroleum, Beijing 102249, P. R. China. E-mail: liub@cup.edu.cn.

† Electronic supplementary information (ESI) available. See DOI: 10.1039/c2jm31541f

the overall storage capacity of the pores through effective use of the pore volume. Another reason we consider doing so is that natural gas always contain water and dehydration is required before adsorption. If our proposal works, this requirement can be removed. In this work, ZIF-8 was selected to verify the feasibility of our idea. We have chosen ZIF-8 because it has high thermal stability as well as good chemical resistance to water.[28] Furthermore, it has been commercialized.

2. Experimental methods

2.1 Experimental apparatus and material

A schematic diagram of the experimental apparatus is shown in Fig. 1. The main parts of the apparatus are a transparent sapphire cell and a steel-made blind cell. They are both installed in an air bath. The effective volume of the sapphire cell is 55.5 cm^3 and the effective volume of the blind cell plus the tubes connecting the two cells is 103.61 cm^3. The designed maximum working pressure of two cells is 20 MPa. The temperature sensor used is a secondary platinum resistance thermometer (type-pt100). A calibrated Heise pressure gauge and differential pressure transducers are used to measure the system pressure. The uncertainties of pressure and temperature measurements are ±0.01 MPa and ±0.1 K, respectively. The changes of the system temperature and pressure with the elapsed time are recorded and displayed by a computer.

Water used in the experiments is double distilled and its conductivity was less than 10^{-4} S m^{-1}. Methane (99.99%) was supplied by Beijing AP Beifen Gases Industry Company Limited. ZIF-8 was obtained from Sigma-Aldrich. The surface area is 1273 m^2 g^{-1} *via* the BET isothermal equation and the micropore volume is 0.61339 cm^3 g^{-1} by the *t*-plot method.[30,31]

2.2 Experimental procedures

2.2.1 Preparation of wet ZIF-8. In our study, wet ZIF-8 with different water content was prepared by the following procedures.

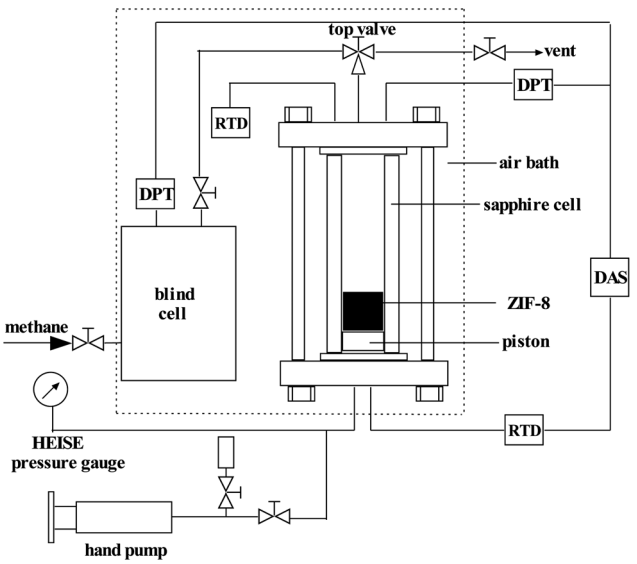

Fig. 1 Schematic diagram of the experimental apparatus. RTD, resistance thermocouple detector; DPT, differential pressure transducer; DAS, data acquisition system.

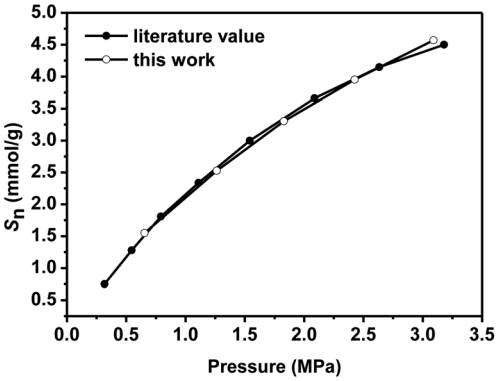

Fig. 2 The comparison of pure CH_4 adsorption isotherm in dry ZIF-8 at 300.15 K measured in this work against that reported in literature.[33]

First, a suitable quantity of purchased ZIF-8 samples was dried at 373.15 K until its mass became constant. Subsequently, it was loaded in a beaker and mixed with water to form a slurry. The beaker containing this slurry was then put in a desiccator and evacuated for more than 5 days to degas the ZIF-8, ensuring the water sufficiently filled the pores. Afterwards, the slurry was dried at 353.15 K. In this way, wet ZIF-8 with different water content was obtained. The percentage mass content of water in wet ZIF-8, x_w, was calculated by the following equation:

$$x_w = \frac{m_w - m_d}{m_w} \times 100\% \quad (1)$$

Where m_w and m_d are the mass of wet and dry ZIF-8, respectively, which were weighed precisely using a balance with a precision of 0.1 mg.

2.2.2 Measurement of storage capacity. The storage capacity of wet ZIF-8 was measured according to the following procedures. At first, the sapphire cell was dismounted from the apparatus, washed with distilled water, dried, and loaded with approximately 10 mL of the prepared wet ZIF-8 of known mass. Subsequently, the cell was installed into the apparatus and connected to the blind cell. The system (sapphire cell + blind cell + tubes connecting two cells) was then purged through vacuuming, replacing with methane, and vacuuming in turn. Afterwards, the top valve of the sapphire cell was closed and the blind cell was charged with methane until the desired pressure was achieved. The air-bath was powered on to adjust the system temperature to the given value. Thereafter, the top valve of the sapphire cell was opened, letting methane flow into the sapphire cell from the blind cell. During the following experimental time period, the top valve was kept open to balance the pressures of the two cells. When the system pressure became constant over a long time (>12 hours) and both the adsorption and the hydrate formation processes were confirmed to be complete, a single experimental run was finished. During each experimental run, the change of pressure with the elapsed time was recorded by a computer. From the recorded *p*–*t* curve one may see two different stages of pressure dropping (see Fig. 6–9). The first stage indicates the adsorption stage and the second one indicates the hydrate formation.

2.2.3 Data processing. The total mole number, n_t, of methane stored by the wet ZIF-8 bed is determined by

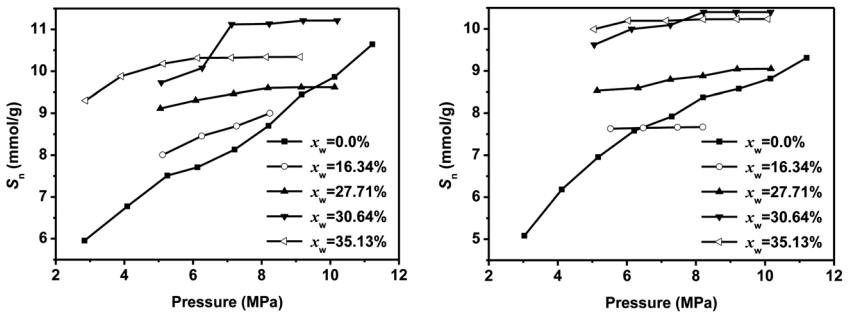

Fig. 3 The variation of net storage capacity of ZIF-8 with pressure (P_1) in the presence of different contents of water at (a) 269.15 K and (b) 274.15 K.

$$n_t = \frac{P_0 V_0}{Z_0 RT} - \frac{P_1 V_1}{Z_1 RT} \quad (2)$$

where T is the system temperature, P_0 is the initial pressure of the blind cell, P_1 is the equilibrium pressure of the system, and R is the gas constant. Compressibility factors Z_0 and Z_1 were calculated using the Peng–Robinson equation of state.[32] V_0 is the total volume of the blind cell plus the tubes connecting two cells. V_1 is the volume of the residual gas, which is defined as

$$V_1 = V_0 + V_s - V_b \quad (3)$$

where V_s is the effective volume of the sapphire cell and V_b is the volume of the wet ZIF-8 particle bed.

The total storage capacity of the ZIF-8 bed in the dry ZIF-8 base, S_t, is defined as

$$S_t = \frac{n_t \times 1000}{m_d} \quad (4)$$

where m_d is the mass of dry ZIF-8.

The volume storage capacity of the ZIF-8 bed, S_v, is defined as

$$S_v = \frac{n_t \times 22400}{V_b} \quad (5)$$

The net mole number, n_p, of methane stored in the pores of ZIF-8 is determined by

$$n_p = \frac{P_0 V_0}{Z_0 RT} - \frac{P_1 V_2}{Z_1 RT} \quad (6)$$

where

$$V_2 = V_0 + Vs - v_d m_d (1 - \varepsilon_d) \quad (7)$$

and v_d is the volume of the dry ZIF-8 bed per unit mass, which was measured to be 2.86 $cm^3 g^{-1}$. ε_d is the bed voidage of the dry ZIF-8.

The net storage capacity of the wet ZIF-8 framework, S_n, excluding the free gas in the void of the ZIF-8 bed is defined as

$$S_n = \frac{n_p \times 1000}{m_d} \quad (8)$$

The volume storage capacity of the ZIF-8 framework, S_{vc}, is defined as

$$S_{vc} = S_n \times 22.4 \times D_c \quad (9)$$

where D_c is the crystallographic density of ZIF-8. It was measured to be 0.9244 $cm^3 g^{-1}$ in this work.

The gas uptake in hydrate formation is determined by

$$n_H = \frac{P_{H0} V_2}{Z_{H0} RT} - \frac{P_1 V_2}{Z_1 RT} \quad (10)$$

where P_{H0} is the pressure at the beginning of hydrate formation and Z_{H0} is the corresponding compressibility factor.

3. Results and discussion

3.1 Blank experiment

In order to check the validity of the experimental method and determine the voidage of the dry ZIF-8 bed, the adsorption

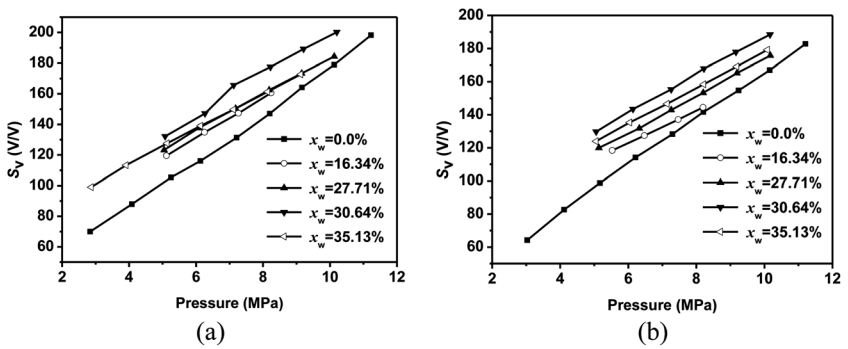

Fig. 4 The variation of overall volume storage capacity of the ZIF-8 bed with pressure (P_1) in the presence of different contents of water at (a) 269.15 K and (b) 274.15 K.

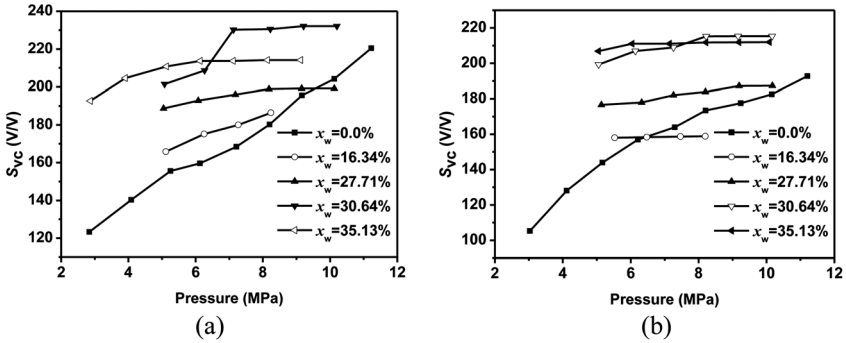

Fig. 5 The variation of volume storage capacity of the ZIF-8 framework with pressure (P_1) in the presence of different contents of water at (a) 269.15 K and (b) 274.15 K.

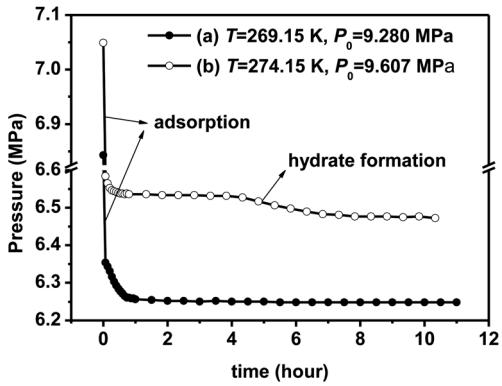

Fig. 6 Adsorption–hydration p–t curves of wet ZIF-8 ($x_w = 16.34\%$).

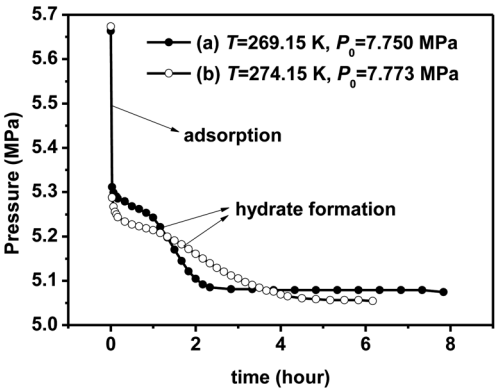

Fig. 8 Adsorption–hydration p–t curves of wet ZIF-8 ($x_w = 30.64\%$).

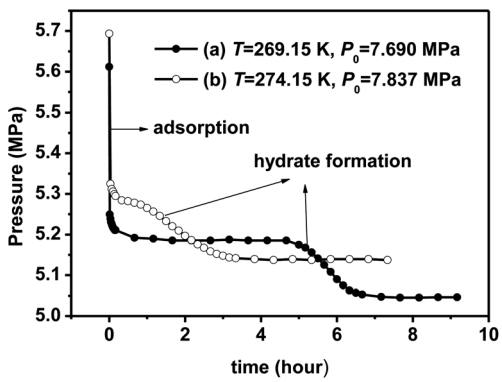

Fig. 7 Adsorption–hydration p–t curves of wet ZIF-8 ($x_w = 27.71\%$).

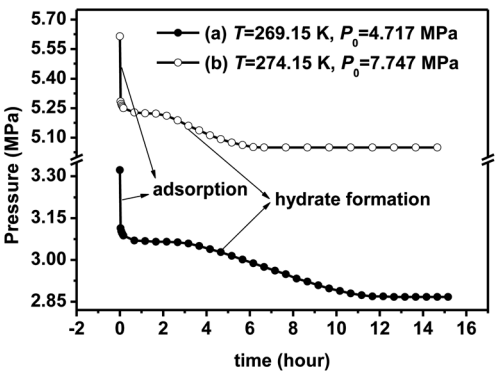

Fig. 9 Adsorption–hydration p–t curves of wet ZIF-8 ($x_w = 35.13\%$).

isotherm of pure CH_4 in dry ZIF-8 at 300.15 K was measured and compared with the literature data.[33] As shown in Fig. 2, we can see the agreement between our experimental results and the literature data is very good. By fitting the experimental data using eqn (6)–(8), the voidage of the dry ZIF-8 bed, ε_d, was determined to be 75%.

3.2 Storage capacity

In order to investigate the effect of the presence of water on the adsorption performance of ZIF-8, a series of experiments were performed to measure the different kinds of storage capacities of

Table 1 Storage capacity of methane hydrate in ZIF-8 pores with different water content

x_w (%)	T (K)	P_1 (MPa)	S_H (V/V)	$n_H/n_p \times 100$ (%)
16.34	274.15	6.474	114.5	16
27.71	269.15	5.046	139.4	35
27.71	274.15	5.139	133.1	33
30.64	269.15	5.077	151.8	38
30.64	274.15	5.054	142.3	36
35.13	269.15	2.867	138.8	45
35.13	274.15	5.049	143.2	43

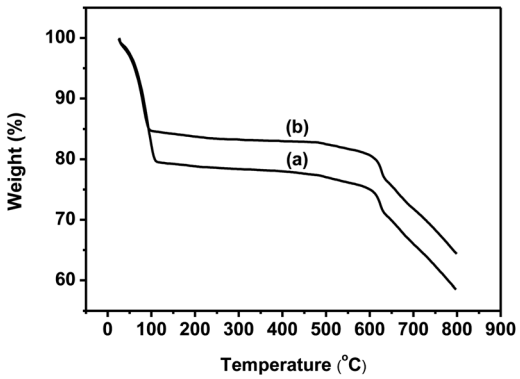

Fig. 10 TGA curves for (a) wet ZIF-8 with $x_w = 31.01\%$ and (b) used wet ZIF-8 with $x_w = 31.01\%$.

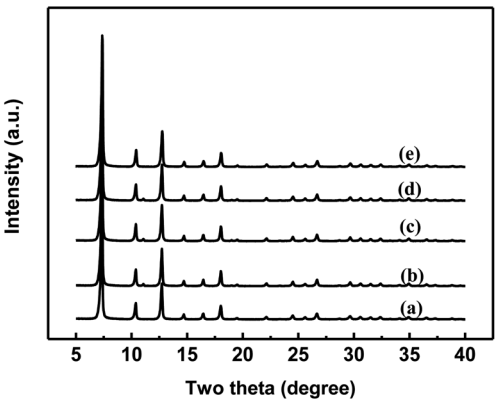

Fig. 12 Powder X-ray diffraction patterns for dry and wet ZIF-8 after adsorption–hydration. (a) Fresh ZIF-8 material, (b) used wet ZIF-8 with $x_w = 16.34\%$, (c) used wet ZIF-8 with $x_w = 27.71\%$, (d) used wet ZIF-8 with $x_w = 30.64\%$, and (e) used wet ZIF-8 with $x_w = 35.13\%$.

wet ZIF-8 under the conditions suitable for hydrate formation, S_t, S_v, S_n, and S_{vc}, which are defined by eqn (4), (5), (8) and (9) respectively. For comparison, the storage capacities of dry ZIF-8 were also measured correspondingly. The water contents of wet ZIF-8 are specified to 16.34%, 27.71%, 30.64%, and 35.13% (mass percentage), respectively. The temperatures were specified to 269.15 K and 274.15 K in order to see the difference in storing behaviors above and below the freezing point of water. The initial pressures were specified to the values under which hydrates can form. The experimental results are shown in Tables S1–S5 in the ESI† and Fig. 3–5, where P_1 is the equilibrium pressure when both adsorption and hydrate formation processes finished. As can be seen from our results, the presence of water in the pores of ZIF-8 increases the storage capacity of ZIF-8 remarkably, regardless of the net storage capacities of the ZIF-8 pores, S_n and S_{vc}, or the overall storage capacities of the ZIF-8 bed, S_t and S_v. For example, at 269.15 K and 2.85 MPa, the net capacity of wet ZIF-8 with a water content of 35.13% is 9.304 mmol g^{-1}, 56% more than that of dry ZIF-8. Correspondingly, the overall volume storage capacity of the ZIF-8 bed increases from 69.94 to 99.01 V/V, a rise of 41.5%. Generally, the extent of the increase in net storage capacity increases with increasing water content. However, for the volume storage capacity of the ZIF-8 bed, S_v, we found there is an optimal water content, *i.e.* 30% or so, at which the highest overall S_v can be achieved. This can be clearly seen in Fig. 4 and may be due to the specific volume of the wet ZIF-8 bed, which was defined as the bed volume per unit mass of dry ZIF-8, changing with different water content. As shown in the bottom of Tables S1–S5 in the ESI†, the specific volumes, v_b, of the wet ZIF-8 bed are 2.86, 2.30, 2.43, 2.41, and 2.75 $cm^3\ g^{-1}$, corresponding to water content of 0.0, 16.34, 27.71, 30.64, and 35.13% respectively. We found v_b decreases from 2.86 to

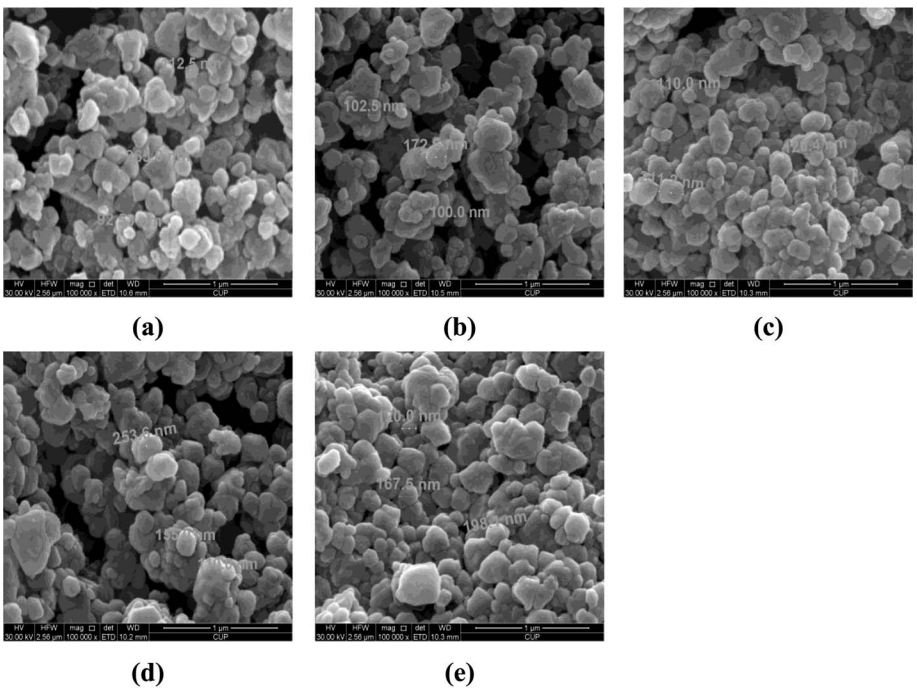

Fig. 11 SEM images for (a) fresh ZIF-8, (b) used ZIF-8 with $x_w = 16.34\%$, (c) used ZIF-8 with $x_w = 27.71\%$, (d) used ZIF-8 with $x_w = 30.64\%$, and (e) used ZIF-8 with $x_w = 35.13\%$.

2.30 $cm^3\ g^{-1}$ first with the presence of water, then it increases with increasing water content. The reason might be attributed to the two effects of water on the ZIF-8 bed. Firstly, the presence of water molecules may make the particles of ZIF-8 more attractive to each other because of the strong hydrogen bond among water molecules. Secondly, water molecules filling the pores may expand the pore volume.[34] The first effect makes v_b decrease while the second one makes it increase with increasing water content.

According to the pore volume of ZIF-8, 0.61339 $cm^3\ g^{-1}$, the maximum water content is 38% when the pore volume is completely filled with water. 35.13% is very close to this value. In this case the pores of ZIF-8 are almost fully filled with water. That is why the maximum water content in our work is 35.13%.

The tendencies of the variations of S_n and S_v with pressure can be clearly seen from Fig. 3 and 4. Unlike dry ZIF-8, the S_n of wet ZIF-8 is not sensitive to pressure, which increases with the increasing of pressure very slowly. At higher pressure, it becomes a constant. This behavior is very similar to that of gas hydrates in storing methane. It implies that all cavities of the hydrate have been filled with methane molecules. It also demonstrates that water or hydrate occupies most of the pore volume and therefore decreases the adsorption capacity which is sensitive to pressure. As to the S_v of the wet ZIF-8 bed, it almost linearly increases with the increasing of pressure. As S_n increases little, the increase of S_v is dominantly attributed to the increase of the capacity of the free void space of the ZIF-8 bed, *i.e.*, it purely results from the compression of the gas. It should be noted that this kind of increase is meaningless as it contributes little to the excess storage capacity over the compression of the gas.

To understand the effect of temperature, we further analyzed the temperature-dependent behavior of S_n and S_v. We found that both S_n and S_v increase with decreasing temperature. But this effect is unremarkable. Thus, considering the feasibility of practical use, relatively high temperature is favorable, only if hydrates can form.

In gas storage processes a good indication of the ability for storage is the volume storage capacity. In this work, the volume storage capacity of the ZIF-8 framework, S_{vc}, was converted from S_n by using the crystallographic density of ZIF-8. As can be seen from Table S5 in the ESI†, S_{vc} of ZIF-8 for methane can achieve 192.63 V/V at 269.15 K and 2.867 MPa, which is less than that of PCN-14 but 7% higher than the DOE target (180 V/V) for methane storage. It should be noted that S_{vc} was converted from the amount of gas adsorbed on the unit mass basis by using crystallographic density. In practice, MOF materials are filled in a tank and the packing factor should be taken into account. Consequently, the actual volume storage capacity would be less than the S_{vc}.[19,21] The pressure-dependent behavior of S_{vc} in both dry and wet ZIF-8 is shown in Fig. 5. Unlike dry ZIF-8, the S_{vc} of wet ZIF-8 increases very slowly with increasing pressure. Overall, we found 5.0 MPa or so is suitable for practical use, under which S_{vc} can achieve more than 200 V/V when a maximum water content of 35% is used.

3.3 Contribution of hydrate to gas uptake

In order to demonstrate the occurrence of hydrate formation in our experiments and display its contribution to total gas uptake, the variation of pressure with the elapsed time was recorded by a computer in each experimental run. Several typical p–t curves are plotted in Fig. 6–9, corresponding to four different water contents, respectively. One can see that there are two different stages of pressure dropping, indicating gas capture in an adsorption process and hydrate formation process, respectively, in most cases. In some cases, there is a distinguishable time period within which the pressure remains a constant between the adsorption stage and the hydrate formation stage, as shown in Fig. 6(b), 7(a), and 9(a) and (b). This time period is called the induction period, which is well-known in the gas-hydrate community. In other cases, the induction period is very short; one can only distinguish the adsorption stage and the hydrate formation stage by finding the transition point of the slope in the p–t curves, as shown in Fig. 7(b) and Fig. 8(a) and (b). The adsorption rate is usually higher than the hydrate formation rate.

The gas uptake attributed to hydrate formation can be determined using eqn (10) if the adsorption stage and hydrate formation stage are distinguishable. The volume storage capacity of the hydrates, S_H, *i.e.* the standard volume of gas stored per volume of hydrate, can then be determined.[35] The determined values of S_H corresponding to the experimental runs depicted in Fig. 6–9 are listed in Table 1. As the adsorption stage and hydrate formation stage are indistinguishable in Fig. 6(a), the corresponding S_H is not shown. From Table 1, we can see that all the S_H values are smaller than the ideal storage capacity of hydrate, *i.e.* 176 V/V. Some the water molecules may form unenclosed cavities which cannot capture gas molecules because the number of water molecules in each pore is largely smaller than that of the bulk hydrate system. The contribution of hydrate to the total gas uptake, n_p, was finally determined from n_H and they are listed in Table 1. One can see the contribution of hydrate to the total uptake of gas increases with the increasing water content. It can achieve as large as 45 percent of the total uptake of gas. These results demonstrate that firstly, hydrates can form in the wet ZIF-8, secondly the increase in the storage capacity of ZIF-8 should be mainly attributed to hydrate formation, and finally wet ZIF-8 can still adsorb gas although its adsorption ability is decreased as water molecules occupy the pore volume.

3.4 Thermal gravimetric analysis (TGA) of the samples

To check if there is still water inside the micropores of ZIF-8 after gas sorption, TGA of the samples was carried out in this work. We used a NETZSCH STA 409 PC/PG instrument, by heating the samples from 25 °C to 800 °C at a rate of 10 °C min^{-1} in an argon flow. Fig. 10 shows the TGA curves of wet ZIF-8 and the used wet ZIF-8 with a water content of 31.01%. From Fig. 10 we can see a gradual weight-loss step of 20.32% and 15.10% up to 100 °C, corresponding to the removal of water molecules from the cavities of the wet ZIF-8 and the used wet ZIF-8, respectively. The weight-loss of the used wet ZIF-8 is less than that of the unused, which might be attributed to the reason that some water in ZIF-8 micropores volatilized during the hydrate decomposition, desorption, and sampling processes. In addition, we found the weight-loss of the unused wet ZIF-8 is less than 31.01%, which might result from the loss of water during the sampling and preparation for the TGA measurement as the quantity of sample used is only 15 mg or so.

3.5 Influence of hydrate formation upon the morphology and crystal structure of ZIF-8

In order to investigate the influence of hydrate formation on the morphology of the particles of ZIF-8, we took SEM images for the ZIF-8 samples studied. Fig. 11 shows the SEM images of fresh ZIF-8 and recovered wet ZIF-8 by decomposing hydrate and desorbing methane at normal pressure and temperature.

From Fig. 11 we can see that for all recovered ZIF-8 with different water contents, there is no remarkable change in the morphology of the particles after a series of processes: saturation with water, adsorption, hydrate formation/decomposition, and desorption in turn. It seems that the presence of water results in the agglomeration among ZIF-8 particles, as shown in Fig. 11 (b)–(e). This may be why the specific bed volume of wet ZIF-8 is smaller than that of the dry one.

For investigating the effect of the series of processes mentioned above on the crystal structure of ZIF-8, XRD analysis was also performed on each of the recovered wet ZIF-8 samples. Before analysis, the samples were dried at 373.15 K until their mass became constant. Powder X-ray diffraction patterns were collected using a SIMADU XRD 6000 diffractometer and Cu K_α radiation (0.1542 nm, 40 kV and 40 mA), scanning at a rate of 2° min^{-1} in the range of 5–40°. As shown in Fig. 12, there is no remarkable change in the crystal structure of ZIF-8. Both SEM measurements and XRD analysis demonstrate that ZIF-8 is stable during the saturation with water and hydrate formation processes, demonstrating it can be used repeatedly.

4. Conclusions

In this work a new method for enhancing the gas storage capacity of MOFs, *i.e.* saturating the MOF with a suitable quantity of water and forming hydrates in it, was proposed. Commercialized ZIF-8 was selected to verify the feasibility of this method. Our experimental results show that hydrates can form in wet ZIF-8 pores and drastically increase methane storage capacities of both ZIF-8 frameworks and ZIF-8 particle beds. Compared with dry ZIF-8, the net storage capacity of a wet ZIF-8 framework with water content of 35.13% is 56% more than that of dry ZIF-8 at 269.15 K and 2.85 MPa. The ideal volume storage capacity of the wet ZIF-8 framework can achieve more than 190 V /V at 3.0 MPa or so, 7% higher than the DOE target (180 V/V) for methane storage. The actual volume storage capacity of the wet ZIF-8 particle bed with the most suitable water content of 30.6% can achieve 150 V/V at 6.5 MPa. In addition, our SEM measurements and XRD analysis demonstrate that ZIF-8 is stable during the saturation and hydrate formation processes, demonstrating it can be used repeatedly.

Applying MOFs for methane storage is one of the most actively studied applications of this class of materials. We think the new approach proposed in this work is of practical significance because not only does it increases the gas storage capacity of MOF drastically, but also it removes the requirement of the dehydration of natural gas before adsorption, which is very energy consuming.

Acknowledgements

The financial support received from the National Natural Science Foundation of China (no. 20925623, 21006126, U1162205), National 973 Project of China (no. 2009CB219504, 2012CB215000), the Research Funds of China University of Petroleum, Beijing (BJBJRC-2010-01), and the Beijing Nova Program (2010B069) are gratefully acknowledged.

References

1 T. Burchell and M. Rogers, *SAE Tech. Pap. Ser.*, 2000, 1653, 2000-01-2205.
2 Z. R. Herm, J. A. Swisher, B. Smit, R. Krishna and J. R. Long, *J. Am. Chem. Soc.*, 2011, **133**, 5664.
3 D. P. Cao, X. R. Zhang, J. F. Chen, W. C. Wang and J. Yun, *J. Phys. Chem. B*, 2003, **107**, 13286.
4 P. Kowalczyk, L. Brualla, A. Żywociński and S. K. Bhatia, *J. Phys. Chem. C*, 2007, **111**, 5250.
5 F. Rodríguez-Reinoso, Y. Nakagawa, J. Silvestre-Albero, J. M. Juárez-Galán and M. Molina-Sabio, *Microporous Mesoporous Mater.*, 2008, **115**, 603.
6 R. Ströbel, J. Garche, P. T. Moseley, L. Jörissen and G. Wolf, *J. Power Sources*, 2006, **159**, 781.
7 A. Celzard and V. Fierro, *Energy Fuels*, 2005, **19**, 573.
8 E. A. Müller, F. R. Hung and K. E. Gubbins, *Langmuir*, 2000, **16**, 5418.
9 K. R. Matranga, A. L. Myers and E. D. Glandt, *Chem. Eng. Sci.*, 1992, **47**, 1569.
10 J. Liu, Y. P. Zhou, Y. Sun, W. Su and L. Zhou, *Carbon*, 2011, **49**, 373.
11 D. P. Cao, W. C. Wang, Z. Shen and J. Chen, *Carbon*, 2002, **40**, 2359.
12 H. Tanaka, M. El-Merraoui, W. A. Steele and K. Kaneko, *Chem. Phys. Lett.*, 2002, **352**, 334.
13 M. Muris, N. Dufau, M. Bienfait, N. Dupont-Pavlovsky, Y. Grillet and J. P. Palmari, *Langmuir*, 2000, **16**, 7019.
14 S. Talapatra, A. Z. Zambano, S. E. Weber and A. D. Migone, *Phys. Rev. Lett.*, 2000, **85**, 138.
15 E. Bekyarova, K. Murata, M. Yudasaka, D. Kasuya, S. Iijima, H. Tanaka, H. Kahoh and K. Kaneko, *J. Phys. Chem. B*, 2003, **107**, 4681.
16 J. A. Dunn, M. Rao, S. Sircar, R. J. Gorte and A. L. Myers, *Langmuir*, 1996, **12**, 5896.
17 A. Chambers, C. Park, R. T. K. Baker and N. M. Rodriguez, *J. Phys. Chem. B*, 1998, **102**, 4253.
18 A. W. Thornton, K. M. Nairn, J. M. Hill, A. J. Hill and M. R. Hill, *J. Am. Chem. Soc.*, 2009, **131**, 10662.
19 H. Wu, W. Zhou and T. Yildirim, *J. Am. Chem. Soc.*, 2009, **131**, 4995.
20 H. Furukawa, N. Ko, Y. B. Go, N. Aratani, S. B. Choi, E. Choi, A. Ö. Yazaydin, R. Q. Snurr, M. O'Keeffe, J. Kim and O. M. Yaghi, *Science*, 2010, **329**, 424.
21 W. Zhou, *Chem. Rec.*, 2010, **10**, 200.
22 A. Martin-Calvo, E. Garcia-Perez, J. M. Castillo and S. Calero, *Phys. Chem. Chem. Phys.*, 2008, **10**, 7085.
23 D. Liu and C. Zhong, *J. Mater. Chem.*, 2010, **20**, 10308.
24 S. Ma, D. Sun, J. M. Simmons, C. D. Collier, D. Yuan and H. C. Zhou, *J. Am. Chem. Soc.*, 2008, **130**, 1012.
25 A. Sayari and Y. Belmabkhout, *J. Am. Chem. Soc.*, 2010, **132**, 6312.
26 J. J. Low, A. I. Benin, P. Jakubczak, J. F. Abrahamian, S. A. Faheem and R. R. Willis, *J. Am. Chem. Soc.*, 2009, **131**, 15834.
27 K. S. Park, Z. Ni, A. P. Côté, J. Y. Choi, R. D. Huang, F. J. Uribe-Romo, H. K. Chae, M. O'Keeffe and O. M. Yaghi, *Proc. Natl. Acad. Sci. U. S. A.*, 2006, **103**, 10186.
28 K. A. Cychosz and A. J. Matzger, *Langmuir*, 2010, **26**, 17198.
29 Z. Q. Hu, Y. F. Chen and J. W. Jiang, *J. Chem. Phys.*, 2011, **134**, 134705.
30 S. Brunauer, P. H. Emmett and E. Teller, *J. Am. Chem. Soc.*, 1938, **60**, 309.
31 J. J. Freeman and A. I. McLeod, *Fuel*, 1983, **62**, 1090.
32 D. Y. Peng and D. B. Robinson, *Ind. Eng. Chem. Fundam.*, 1976, **15**, 59.
33 H. C. Guo, F. Shi, Z. F. Ma and X. Q. Liu, *J. Phys. Chem. C*, 2010, **114**, 12158.
34 J. P. Pellitero, H. Amrouche, F. R. Siperstein, G. Pirngruber, C. N. Draghi, G. Chaplais, A. S. Masseron, D. B. Bachi, D. Peralta and N. Bats, *Chem.–Eur. J.*, 2010, **16**, 1560.
35 W. Lin, G. J. Chen, C. Y. Sun, X. Q. Guo, Z. K. Wu, M. Y. Liang, L. T. Chen and L. Y. Yang, *Chem. Eng. Sci.*, 2004, **59**, 4449.

